Energy & Environmental Science

COMMUNICATION

View Article Online
View Journal | View Issue

Formamidinium lead trihalide: a broadly tunable perovskite for efficient planar heterojunction solar cells†

Cite this: *Energy Environ. Sci.*, 2014, 7, 982

Received 22nd November 2013
Accepted 3rd January 2014

DOI: 10.1039/c3ee43822h

www.rsc.org/ees

Giles E. Eperon, Samuel D. Stranks, Christopher Menelaou, Michael B. Johnston, Laura M. Herz and Henry J. Snaith*

Perovskite-based solar cells have attracted significant recent interest, with power conversion efficiencies in excess of 15% already superceding a number of established thin-film solar cell technologies. Most work has focused on a methylammonium lead trihalide perovskites, with a bandgaps of ~1.55 eV and greater. Here, we explore the effect of replacing the methylammonium cation in this perovskite, and show that with the slightly larger formamidinium cation, we can synthesise formamidinium lead trihalide perovskites with a bandgap tunable between 1.48 and 2.23 eV. We take the 1.48 eV-bandgap perovskite as most suited for single junction solar cells, and demonstrate long-range electron and hole diffusion lengths in this material, making it suitable for planar heterojunction solar cells. We fabricate such devices, and due to the reduced bandgap we achieve high short-circuit currents of >23 mA cm^{-2}, resulting in power conversion efficiencies of up to 14.2%, the highest efficiency yet for solution processed planar heterojunction perovskite solar cells. Formamidinium lead triiodide is hence promising as a new candidate for this class of solar cell.

Broader context

Within the past 2 years, hybrid organic–inorganic perovskite solar cells have shot up to efficiencies of over 15%, eclipsing several more established thin-film technologies. These solar cells are solution-processable, cheap and use only earth-abundant materials, making them a prime contender for high efficiency, low-cost solar power generation. The majority of these advances have used methylammonium lead trihalide, a perovskite semiconductor that does not absorb as much of the solar spectrum as an optimum single-junction solar cell should – it is limited by its bandgap of ~1.55 eV, whereas the optimum would be 1.1–1.4 eV. Here, we push this closer to the optimum; by replacing the methylammonium component with a slightly larger cation, formamidinium, which reduces the bandgap of the perovskite to 1.48 eV, allowing greater spectral absorption. Furthermore, we demonstrate that this material has favourable charge transport characteristics, allowing it to be incorporated into the simplest device architecture, composed of a solid thin absorber layer of perovskite sandwiched between two charge selective contacts. We fabricate such solar cells with formamidinium lead triiodide, and find that the reduced bandgap allows very high currents to be generated under simulated sunlight. As such, we achieve record efficiencies for solution processed planar heterojunction perovskite solar cells, and demonstrate the potential for solar cells incorporating this material to become the leading contenders in this new field.

Over the last two years, hybrid organic–inorganic perovskite solar cells have distinguished themselves as an impressively efficient, inexpensive technology.[1] Power conversion efficiencies have shot up to over 15% by utilising methylammonium lead trihalide perovskite.[2,3] This material is a solution-processable semiconductor, which has a bandgap of approximately 1.55 eV, giving light absorption across most of the solar spectrum, up to a wavelength of ~800 nm.[4,5] Additionally, a previous study has shown that by varying the halide composition between iodide and bromide in this material, the bandgap can be tuned between 1.55 and 2.3 eV, enabling variation in colour and optimisation for applications in multi-junction solar cells.[6] However, it is known that the optimal bandgap for a single-junction solar cell is between 1.1 and 1.4 eV, currently beyond the range of the methylammonium lead trihalide system.[7] In addition, for the bottom cell in a tandem architecture, the optimum band gap is around 1 eV, giving good motivation to realise lower band gap perovskite absorbers.[7] As we illustrate in Fig. 1a, perovskites are defined as any compound which crystallises in the ABX_3 structure, consisting of corner-sharing BX_6 octahedra with the A component neutralising total charge. In the case of the organometal trihalide perovskites, A is an organic cation, B is the metal cation, and X a halide anion. Methylammonium lead triiodide, the perovskite of most recent interest, has a tetragonal perovskite structure arising from a distortion of the perovskite lattice.[8] It has been proposed that in this system, the organic A cation does not play a major role in determining the band structure, and acts to fulfil charge neutrality within the lattice.[9] Nevertheless, its size is important. A larger or smaller A cation can cause the whole lattice to expand or contract. Changing the B–X bond length has been

Department of Physics, University of Oxford, Clarendon Laboratory, Parks Road, Oxford, OX1 3PU, UK. E-mail: h.snaith1@physics.ox.ac.uk

† Electronic supplementary information (ESI) available: Experimental methods, supplementary data and details of calculations. See DOI: 10.1039/c3ee43822h

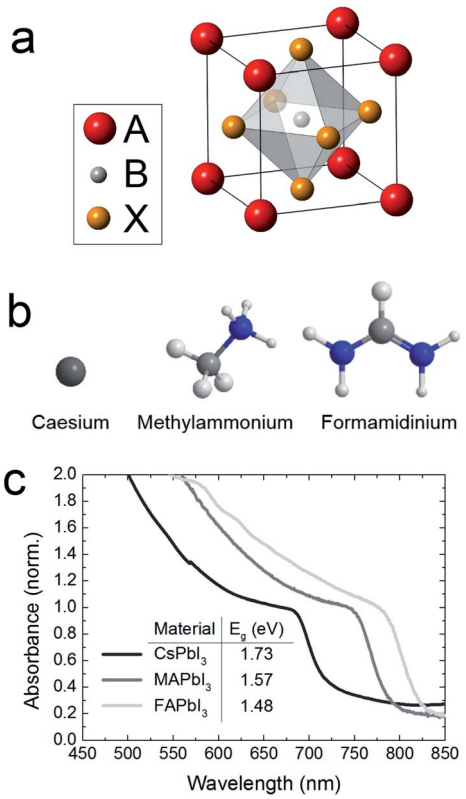

Fig. 1 Tuning perovskite bandgap by replacing the A cation. (a), The ABX_3 perovskite crystal structure. (b) The atomic structure of the three A site cations explored. (c) UV-Vis spectra for the $APbI_3$ perovskites formed, where A is either caesium (Cs), methylammonium (MA) or formamidinium (FA).

demonstrated to be important in determination of bandgap.[6] Motivated by this, we therefore investigated whether the bandgap could be tuned in a similar way by variation of the A cation size. Given a particular metal and halide, there is a relatively small size range allowed for the A cation, since it must fit between the corner-sharing metal halide octahedra. If it is too large, the 3D perovskite structure is unfavourable; lower-dimensional layered or confined perovskites will be formed.[8] If too small, the lattice would be too strained to form. A so-called tolerance factor has been defined previously, to describe the limits on ionic sizes of each component, as detailed in the ESI.†[8] The larger ethylammonium cation has been explored previously in solar cells, and was shown to form a wider bandgap perovskite due to a 2H-type structural rearrangement – it was too large to maintain the 3-dimensional tetragonal ABX_3 lattice.[10]

Here, we investigate the impact of tuning the size of the A cation, in order to push the bandgap of the perovskite absorber further towards the infrared. We find that an increase in the cation size results in a reduction in the band gap and we are able to fabricate solar cells employing formamidinium lead triiodie that convert to current a greater proportion of the sun's spectrum. We fabricate high efficiency solution-processed planar heterojunction solar cells, demonstrating power conversion efficiencies of up to 14.2%. To the best of our knowledge, this is the first report of formamidinium lead trihalide-based solar cells.

To investigate the effect of the A cation size upon the optical and electronic properties of the perovskite, we synthesised perovskites based on methylammonium lead triiodide, replacing methylammonium ($CH_3NH_3^+$)(MA) with caesium (Cs^+) and formamidinium ($HC(NH_2)_2^+$) (FA), illustrated in Fig. 1b. Caesium has a smaller effective ionic radius compared to methylammonium, whereas formamidinium is slightly larger.[9] We use a single precursor solution to spin-coat onto substrates; the perovskite then forms upon heating. Full experimental details are provided in the ESI.† Previous studies have reported the synthesis of these materials in crystalline form, but to our knowledge this is the first report of their thin-film synthesis using a single precursor spin-coating route.[11–14] We show the absorbance spectra of these materials in Fig. 1c.

We observe that caesium lead triiodide absorbs up to a shorter wavelength, whereas formamidinium lead triiodide absorbs to a longer wavelength than methylammonium lead triiodide. Estimations of the bandgap from Tauc plots (described in full in the ESI†) gives values shown as an inset in Fig. 1c. We observe that as the A cation increases in ionic radius, and hence the lattice would be expected to expand, the bandgap decreases, causing a red-shift in the absorption onset. Just by replacing the methylammonium with the slightly larger formamidinium, we are able to shift the bandgap closer to the optimum for a single junction solar cell.[7] As such, this material is a likely candidate to be able to produce even more efficient solar cells than $MAPbI_3$.

We fabricated a range of formamidinium lead bromide-iodide mixed halide perovskites ($FAPbI_yBr_{3-y}$) to explore the range of bandgap tunability of the formamidinium lead trihalide system. We were able to form most fractional mixtures, but we note that we were unable to form crystalline phases (as determined by X-ray diffraction (XRD)) for $y = 0.5$, 0.6 and 0.7, so these are not detailed here. The absorbance and photoluminescence from the perovskites in this series are shown in Fig. 2a and b respectively. Extracting the bandgap from Tauc plots, we determine that the bandgap is tunable between 1.48 and 2.23 eV, providing a whole range of coloured perovskites, as illustrated in Fig. 2c. An increase in iodide fraction gradually red-shifts the bandgap. Photoluminescence peaks correspond well to the absorption onsets, suggesting the observed photoluminescence is predominantly from the bandgap rather than trap or sub-band states.[15] As observed for the methylammonium lead trihalide system previously studied,[6] analysis of XRD data (shown in full in the ESI†) shows that the perovskites transition from a cubic (for $y < 0.5$, Br-rich) to a tetragonal ($y > 0.7$, I-rich) crystal structure. Fig 2d shows the shift of the [100] (cubic) to the equivalent [110] (tetragonal) peak for these perovskites. A gradual shift in the lattice spacing upon increasing the iodide fraction is observed. Because the tetragonal symmetry arises from octahedral tilting, as illustrated in the ESI,† we are able to describe a tetragonal perovskite lattice with a 'pseudocubic' lattice parameter that allows comparison with cubic lattices, as described in the literature and detailed in the ESI.†[6] Determining the pseudocubic lattice parameter a^* for the tetragonal-

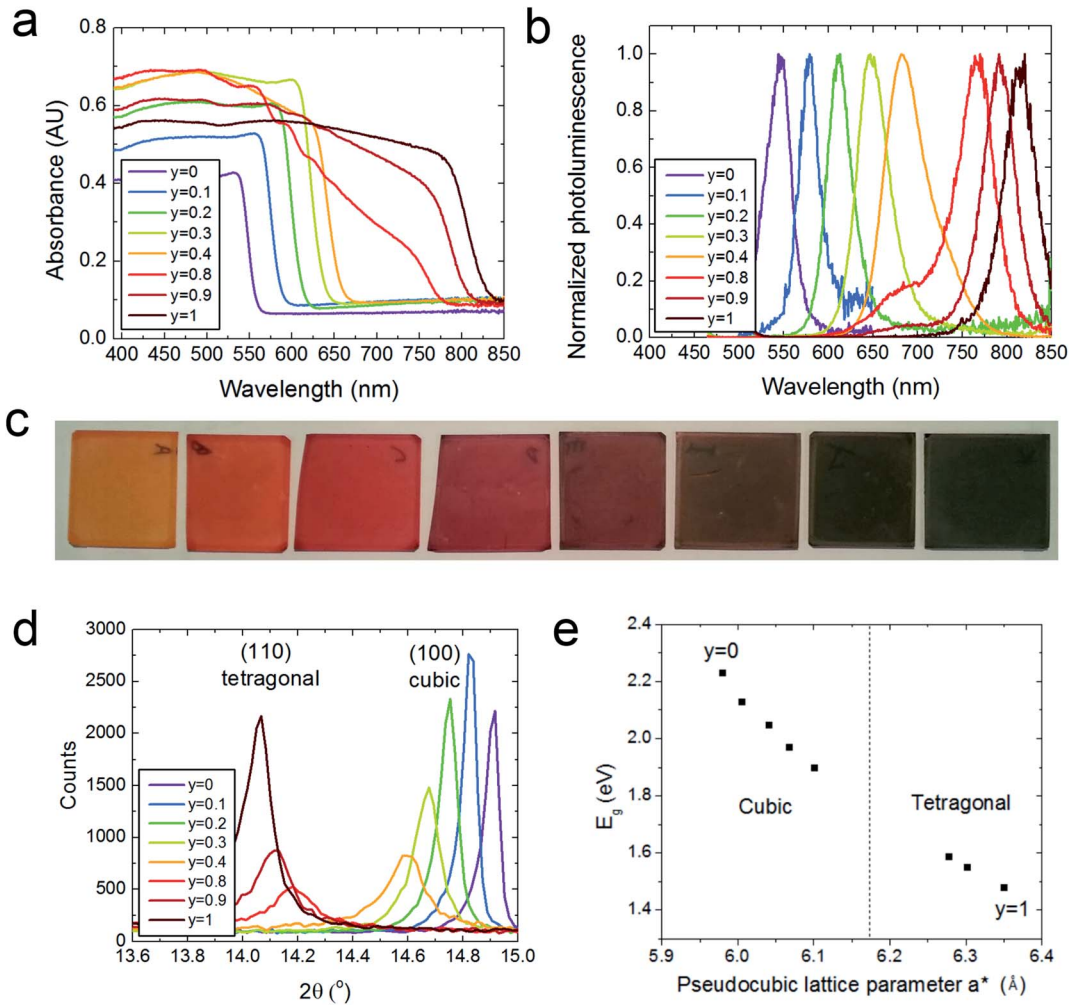

Fig. 2 Tunability of the $FAPbI_yBr_{3-y}$ perovskite system. (a) UV-Vis absorbance of the $FAPbI_yBr_{3-y}$ perovskites with varying *y*, measured in an integrating sphere. (b) Corresponding steady-state photoluminescence spectra for the same films. (c) Photographs of the $FAPbI_yBr_{3-y}$ perovskite films with *y* increasing from 0 to 1 (left to right). (d) XRD spectra of $FAPbI_yBr_{3-y}$ films showing the shift of the 100 (cubic) perovskite peak to the (110) tetragonal peak as *y* decreases. (e) Variation of bandgap with pseudocubic lattice parameter as determined from XRD spectra.

phase perovskites, and cubic lattice parameter *a* (directly comparable to *a**) for the cubic perovskites enables us to plot the relation between bandgap and lattice spacing for this system. As we show in Fig. 2e, we observe that a larger pseudocubic lattice parameter results in a narrower bandgap. The relationship appears continuous across the phase change. This tunability shows that the new formamidinium system has wide flexibility; further investigation of the properties of the whole range of coloured perovskites may prove very interesting, specifically for optimising a wider band gap perovskite for a top cell in a tandem solar cell architecture.

Formamidinium lead iodide shows a narrower bandgap than the commonly used methylammonium lead iodide, 1.48 eV (~840nm absorption onset) compared to ~1.57 eV respectively, and hence lies closer to that favourable for optimum solar conversion efficiencies. We should be able to attain higher photocurrents by harnessing more of the solar spectrum, provided the photogenerated electrons and holes are suitably mobile and suitably long lived to be efficiently extracted from the solar cell. Previous reports on perovskite solar cells have explored four main architectures. Firstly, the 'sensitizing' architecture, where the perovskite simply acts as an absorber coating mesoporous TiO_2, with excited carriers injected into hole and electron transporting media for collection at the electrodes.[3–5,16] Secondly, the meso-superstructured architecture, where an inert scaffold forces electron transport through the perovskite itself.[16,17] Thirdly, the hole-conductor-free architecture, where in a similar way the removal of a separate hole transporter means that all hole transport occurs through the perovskite.[18,19] Finally, a bulk thin-film architecture with planar heterojunctions has most recently shown the highest efficiencies; here a bulk layer of perovskite is both absorber and long-range transporter of both charge species.[2,15,20] The thin-film and mesostructured approaches should ultimately provide the highest efficiencies, since the interfacial area at the heterojunction is minimised, where non-radiative recombination losses are most likely to occur. However, for a material to function well in the planar heterojunction configuration, it

must be able to transport charge across film thicknesses greater than the absorption depth of a few hundred nanometers. To determine the optimum architecture for incorporation of $FAPbI_3$ into photovoltaic devices, whether thin-film, meso-superstructured or sensitizing, we conducted time resolved photoluminescence quenching experiments using the technique described in detail in previous work by ourselves and others, to obtain values for the electron and hole effective diffusion lengths.[15,21–23] In brief, we spin-coat a hole (2,2′,7,7′-tetrakis-(*N*,*N*-di-*p*-methoxyphenylamine)9,9′-spirobifluorene, spiro-OMeTAD) or electron (phenyl-C61-butyric acid methyl ester, PCBM) quenching layer on top of a continuous thin film of the perovskite. Electrons or holes that diffuse into the boundary between perovskite and the quencher, transfer to the quencher and can no longer contribute to photoluminescence. By measuring the time-resolved photoluminescence decay rate with and without a quencher, and fitting the observed behaviour to a diffusion equation, we can estimate a diffusion length for the charge carrying species.[15]

Notably, it is important to carry out these measurements on very uniform and continuous thin films of the material in question. Spin-coating the formamidinium iodide (FAI) plus PbI_2 precursor solution in *N*,*N*-dimethylformamide (DMF) initially resulted in discontinuous perovskite films. However, as shown in Fig. 3a and b, we found that by adding a small amount of hydroiodic acid (HI) to the stoichiometric FAI : PbI_2 1 : 1 perovskite precursor solution, we could form extremely uniform and continuous films, with phase purity verified by XRD (see ESI†), which is in good agreement with previous reports on the crystal structure of this perovskite.[11] We note that after annealing these thin films we do not observe any significant presence of the previously reported "yellow phase".[11] Moreover, realising a highly uniform coating is likely to have a beneficial effect on device performance; the highest efficiency perovskite solar cells reported to date were fabricated *via* thermal evaporation, the main advantage thought to be that this method delivers a continuous and uniform pinhole-free layer.[2] With the addition of the acid to the formamidinium perovskite precursor solution, we have found a simple way to form a pinhole-free continuous film using conventional solution-processing. This method has, to the best of our knowledge, not been reported before. We propose that adding acid helps to solubilise the inorganic component, and so slows down crystallization of the film upon spin-coating, enabling a smoother film to be formed, without having any impact on the crystal structure, as verified by XRD (see ESI†). We found that in the same way, addition of HI to a highly concentrated solution of lead iodide in DMF considerably enhanced its solubility. This simple technique should prove very useful as a general method for preparing very smooth hybrid organic–inorganic films, or preparing more concentrated precursor solutions.

We verified that PCBM and Spiro-OMeTAD are effective quenching layers for electrons and holes respectively by measuring the steady-state photoluminescence spectra of perovskite films with these quenchers on top. As shown in the ESI,† both quenchers are effective, however the PCBM does not entirely quench the PL from $FAPbI_3$, in contrast to nearly complete quenching when coated upon $MAPbI_3$.[15] As we show in Fig. 3c, by monitoring the time-resolved photoluminescence intensity at the peak wavelength (810 nm), we were able to estimate effective diffusion lengths for electrons and holes in this material, as 177 ± 20 nm and 813 ± 72 nm respectively. As shown in the ESI,† we find that films of a few hundred nanometers thickness have sufficient optical density to absorb most incident light in two passes and as such, a thin-film planar heterojunction should be able to provide both efficient hole and electron extraction and light absorption, making this a suitable configuration for $FAPbI_3$ solar cells. We note that both the

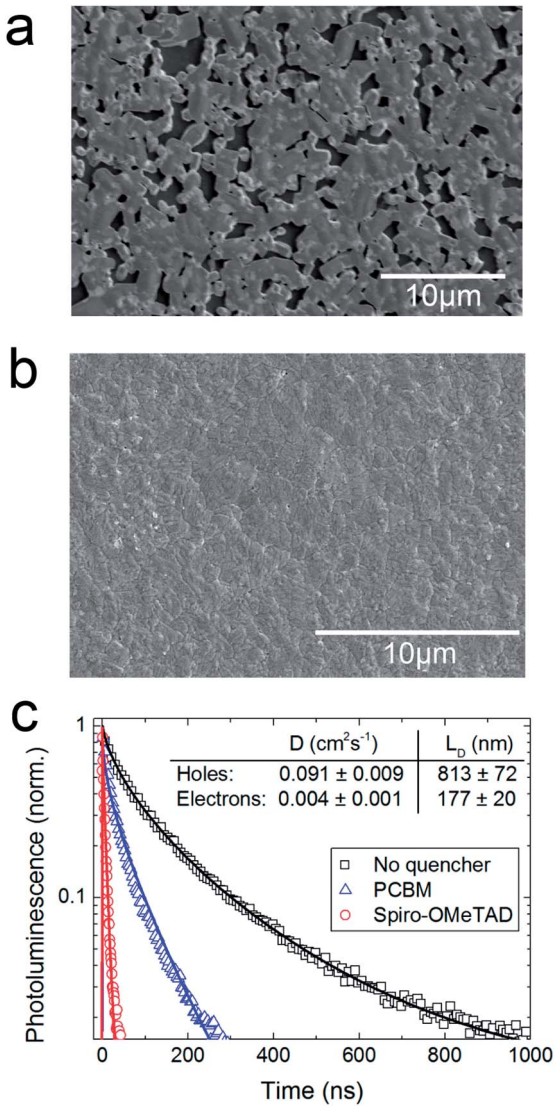

Fig. 3 Time-resolved photoluminescence quenching measurements on smooth $FAPbI_3$ films. Top view scanning electron micrograph of the sample morphology of a $FAPbI_3$ film formed from spin-coating the precursor solution with (a) no addition of hydroiodic acid, and (b) with adding a small amount of hydroiodic acid to the same precursor just before spin-coating. (c) Normalised time-resolved photoluminescence intensity from films with and without electron and hole-quenchers, showing the stretched exponential fits to the decay curves. Diffusion coefficients (D) and diffusion lengths (L_D), extracted from the fitting, are shown in the inset. Errors quoted arise predominantly from film thickness variations.

diffusion length for holes and electrons are significantly longer than those found in $MAPbI_3$, but shorter that those in the mixed halide $MAPbI_{3-x}Cl_x$ perovskite, which are over 1 micron for both electrons and holes.[15] Interestingly, there appears to be a significant imbalance in the electron and hole diffusion lengths. This arises from a lower determined diffusion coefficient for electrons, as shown in Fig. 3c, rather than a reduced lifetime. We do not have conclusive evidence for any particular mechanism giving rise to the imbalance, but propose that by replacing methylammonium with formamidinium, the band structure of the perovskite is altered, giving rise to an imbalance in the effective masses for electron and hole. This would in turn affect the diffusion coefficient and hence the diffusion length. We also note however, that the diffusion length modelling assumes perfect quenching, *i.e.* that once a charge species meets the interface with a quencher it transfers to the quencher with 100% efficiency and is not reflected. If the PCBM is not an ideal electron acceptor for the $FAPbI_3$, then the estimation of the electron diffusion coefficient and length is a lower limit.

We fabricated and optimised thin-film planar heterojunction solar cells with the $FAPbI_3$ perovskite, using compact TiO_2 and Spiro-OMeTAD as electron- and hole-selective contacts respectively. The device architecture is shown in Fig. 4a. We measured current–voltage characteristics of such devices under simulated air-mass (AM)1.5 100 mW cm^{-2} sun light, and show these characteristics for the best device fabricated, and for the numerical mean of a 24 cell batch, in Fig. 4b. Full details of device performance for the whole batch of such devices is detailed in the ESI.† Due to the high short-circuit currents of over 23 mA cm^{-2}, we observe power conversion efficiencies in the best performing devices of up to 14.2%, making this a new record for solution-processed planar heterojunction perovskite solar cells. As shown in the EQE spectrum (Fig. 4c), we are able to generate photocurrent out to ~840nm, rather than only ~800 nm achievable with the well-known $MAPbI_3$ material, due to the narrower bandgap.[3] The integration of the measured EQE spectrum over the solar spectrum estimates a short-circuit current density of 18.2 mA cm^{-2}, close to the average photocurrent generated from a typical cell. We note that this EQE spectrum is taken from a representative device from the batch, not the champion device.

The high power conversion efficiency in this system can be explained by two main advantages of the $FAPbI_3$ perovskite. Firstly, we are able *via* solution-processing to form a very uniform and continuous thin film, with very few pinholes or defects, which has been a difficult challenge for the $MAPbX_3$ films.[20] Uniform perovskite coverage is likely to lead to maximising the V_{oc}. Secondly, the reduced bandgap of 1.48 eV compared to ~1.57 eV in the $MAPbI_{3-x}Cl_x$ perovskite allows absorption of photons over a greater proportion of the solar spectrum, and is closer to the ideal bandgap for a single-junction solar cell. We would expect a corresponding drop in V_{oc} to accompany a smaller bandgap. The V_{oc} attained in the best $FAPbI_3$ planar heterojunction solar cells is 0.94 V, compared to 0.97 V observed in the best $MAPbI_{3-x}Cl_x$ solution-processed planar heterojunction solar cells.[15] The reduction in bandgap from $MAPbI_{3-x}Cl_x$ to $FAPbI_3$ is ~0.09 eV, whereas the V_{oc} only drops by 0.03 V, so in these cells we actually observe a lower voltage loss from optical bandgap to V_{oc} (loss-in-potential) than in the $MAPbI_{3-x}Cl_x$ cells – 0.54 eV compared with ~0.58 eV. This implies fewer energetic losses, as a result of the highly uniform films or for another reason.

We note that by employing a meso-superstructred approach, even higher voltages of up to ~1.1 V have been observed in the $MAPbI_{3-x}Cl_x$ system.[16] The origin of these higher voltages in comparison to the solution processed planar heterojunction devices are yet to be understood fully, but the loss-in-potential is only ~0.45 eV, even lower than the loss in the $FAPbI_3$ cells. If we can further reduce this loss in the $FAPbI_3$ by, for instance, employing a mesostructure, a more appropriate choice or energetically tuning of the n- and p-type collection layers, or by enhancing the electron diffusion length with halide doping, then even higher efficiencies should be possible with formamidinium lead trihalide.

Having fabricated high-efficiency $FAPbI_3$ devices, it is now of interest to observe how devices fabricated with the increased bromide fractions function. Having higher bandgaps, they should be able to generate higher open-circuit voltages, as previously shown with the $MAPbX_3$ system.[24,6] To explore this, we fabricated planar heterojunction solar cells in the same way with two further compositions of $FAPbI_yBr_{3-y}$ perovskites, $y = 0$ ($FAPbBr_3$) and $y = 0.8$ (small replacement of iodide with bromide). Current–voltage characteristics of the best devices of these compositions fabricated are shown in Fig. 4d, as compared to the best $FAPbI_3$ device. We observe that by decreasing the iodide fraction (increasing the bromide fraction) from $y = 1$ to $y = 0.8$, we are able to generate higher open-circuit voltages of 1.0 V, accompanying a drop in photocurrent. This corresponds to a change in bandgap from 1.48 eV to 1.55 eV, so the increase in V_{oc} is more or less what we would expect assuming no further energetic losses. Increasing the bromide fraction further by going all the way to $FAPbBr_3$, however, we observe that the V_{oc} increases only slightly further, to 1.02 V. Here the bandgap is now 2.23 eV, so the V_{oc} increase is much less than the bandgap increase. Something else must then be limiting the V_{oc}. We propose that this is the HOMO level of the Spiro-OMeTAD hole transporter. Unless we were to use a different hole transport material, with a deeper HOMO level, the voltage of such devices is likely to be limited to just above 1 V.

A fundamental property of the methylammonium lead iodide perovskite is that it is sensitive to degradation due to moisture and high temperatures.[6,11] Though this is likely to be manageable in manufacture, any modifications which enhance the robustness of the material will be advantageous. We carried out some initial tests to determine how replacing the methylammonium cation with formamidinium affects these important properties. We found that formamidinium lead iodide is more resistant when exposed to high temperatures in air than methylammonium lead iodide – it seems fully stable without discolouration at 150 °C in air, whereas the methylammonium-based perovskite discoloured after ~30 minutes (see ESI Fig. S7†). Exposing the perovskites to a moist atmosphere did result in degradation of the formamidinium perovskite at a

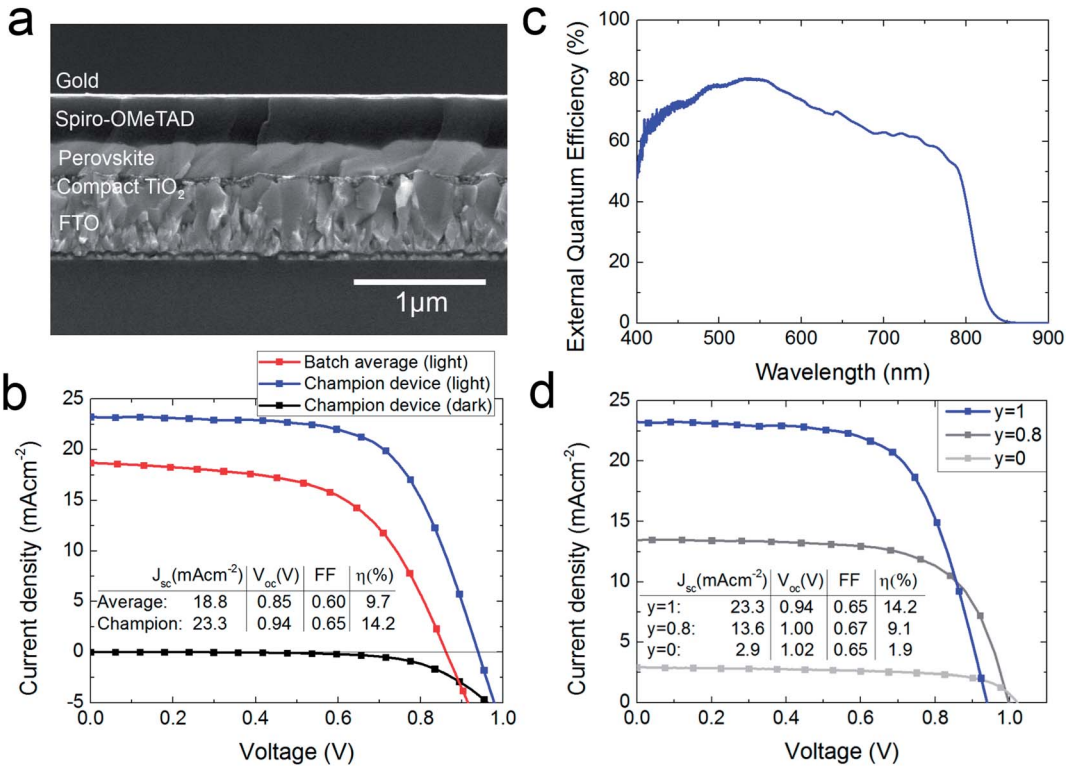

Fig. 4 Planar heterojunction $FAPbI_3$ solar cells. (a) Cross-sectional scanning electron micrograph of a representative $FAPbI_3$ device. (b) Current–voltage characteristics of $FAPbI_3$ planar heterojunction solar cells under 100 mW cm^{-2} AM1.5 illumination, showing both the mean current–voltage characteristics for the batch of 24 cells detailed in the ESI† and the current–voltage characteristics of the champion device fabricated. Performance parameters are shown as an inset. (c) External quantum efficiency spectrum of a representative $FAPbI_3$ solar cell. (d) Current–voltage characteristics of $FAPbI_yBr_{3-y}$ planar heterojunction solar cells under 100 mW cm^{-2} AM1.5 illumination, showing devices with $y = 0.8$ and $y = 0$ compared to the champion $FAPbI_3$ solar cell. Performance parameters are shown as an inset.

similar rate to the methylammonium perovskite (ESI Fig. S8†). However, recent work on long-term stability of perovskite solar cells shows promise that with adequate encapsulation, similar devices to these can function continuously under illumination for thousands of hours, so this is unlikely to be a significant drawback to commercialisation of perovskite solar cells such as these.[25,3] Furthermore, the enhanced temperature stability is an extremely promising property, possibly indicative of better long-term thermal durability, and will be the subject of further investigations.

Conclusion

We investigated the effect of changing the size of the A cation in the organolead trihalide perovskite structure, and found that we are able to tune the bandgap in this manner. We showed that replacing methylammonium with formamidinium narrows the bandgap, enabling broad bandgap tunability with the mixed halide $FAPbI_yBr_{3-y}$ perovskite system between 1.48 and 2.23 eV. Since $FAPbI_3$ displays a bandgap of 1.48 eV, it is closer to the 'ideal' single-junction solar cell bandgap of between 1.1 and 1.4 eV. To determine the optimum device configuration, we carried out spectroscopic diffusion length measurements, determining that $FAPbI_3$ has sufficiently long electron and hole diffusion lengths for planar heterojunction solar cells to be a suitable configuration. We fabricated such cells, and due to the reduced bandgap of $FAPbI_3$ we observed very high short-circuit currents in excess of 23 mA cm^{-2} and achieved up to 14.2% power conversion efficiency, as measured under simulated full sun light. This firmly places formamidinium metal trihalide perovskites as a contending class of materials for high efficiency solar cells.

Acknowledgements

We would like to thank Elizabeth Parrott for assistance with photoluminescence quenching measurments, and Nakita K. Noel and James M. Ball for helpful discussions. This work was supported by EPSRC and Oxford Photovoltaics Ltd. through a Nanotechnology KTN CASE award, and the European Research Council (ERC) HYPER PROJECT no. 279881.

Notes and references

1 H. J. Snaith, *J. Phys. Chem. Lett.*, 2013, **4**, 3623–3630.
2 M. Liu, M. B. Johnston and H. J. Snaith, *Nature*, 2013, **501**, 395–398.
3 J. Burschka, N. Pellet, S.-J. Moon, R. Humphry-Baker, P. Gao, M. K. Nazeeruddin and M. Grätzel, *Nature*, 2013, **499**, 316–319.

4 H.-S. Kim, C.-R. Lee, J.-H. Im, K.-B. Lee, T. Moehl, A. Marchioro, S.-J. Moon, R. Humphry-Baker, J.-H. Yum, J. E. Moser, M. Grätzel and N.-G. Park, *Sci. Rep.*, 2012, **2**(591), 1–7.
5 A. Kojima, K. Teshima, Y. Shirai and T. Miyasaka, *J. Am. Chem. Soc.*, 2009, **131**, 6050–6051.
6 J. H. Noh, S. H. Im, J. H. Heo, T. N. Mandal and S. Il Seok, *Nano Lett.*, 2013, **13**, 1764–1769.
7 F. Meillaud, A. Shah, C. Droz, E. Vallat-Sauvain and C. Miazza, *Sol. Energy Mater. Sol. Cells*, 2006, **90**, 2952–2959.
8 D. B. Mitzi, *Progress in Inorganic Chemistry*, John Wiley & Sons, Inc, 1999, vol. 48.
9 I. Borriello, G. Cantele and D. Ninno, *Phys. Rev. B: Condens. Matter Mater. Phys.*, 2008, **77**, 235214.
10 J.-H. Im, J. Chung, S.-J. Kim and N.-G. Park, *Nanoscale Res. Lett.*, 2012, **7**, 353.
11 C. C. Stoumpos, C. D. Malliakas and M. G. Kanatzidis, *Inorg. Chem.*, 2013, **52**, 9019–9038.
12 O. N. Yunakova, V. K. Miloslavskii and E. N. Kovalenko, *Opt. Spectrosc.*, 2012, **112**, 91–96.
13 D. M. Trots and S. V. Myagkota, *J. Phys. Chem. Solids*, 2008, **69**, 2520–2526.
14 G. Murtaza and I. Ahmad, *Phys. B*, 2011, **406**, 3222–3229.
15 S. D. Stranks, G. E. Eperon, G. Grancini, C. Menelaou, M. J. P. Alcocer, T. Leijtens, L. M. Herz, A. Petrozza and H. J. Snaith, *Science*, 2013, **342**, 341–344.
16 M. M. Lee, J. Teuscher, T. Miyasaka, T. N. Murakami and H. J. Snaith, *Science*, 2012, **338**, 643–647.
17 J. M. Ball, M. M. Lee, A. Hey and H. J. Snaith, *Energy Environ. Sci.*, 2013, **6**, 1739–1743.
18 W. A. Laban and L. Etgar, *Energy Environ. Sci.*, 2013, **6**, 3249–3253.
19 L. Etgar, P. Gao, Z. Xue, Q. Peng, A. K. Chandiran, B. Liu, M. K. Nazeeruddin and M. Grätzel, *J. Am. Chem. Soc.*, 2012, **134**, 17396–17399.
20 G. E. Eperon, V. M. Burlakov, P. Docampo, A. Goriely and H. J. Snaith, *Adv. Funct. Mater.*, 2013, **24**, 151–157.
21 G. Xing, N. Mathews, S. Sun, S. S. Lim, Y. M. Lam, M. Gratzel, S. Mhaisalkar and T. C. Sum, *Science*, 2013, **342**, 344–347.
22 P. E. Shaw, A. Ruseckas and I. D. W. Samuel, *Adv. Mater.*, 2008, **20**, 3516–3520.
23 D. Markov and P. Blom, *Phys. Rev. B: Condens. Matter Mater. Phys.*, 2006, **74**, 085206.
24 B. Cai, Y. Xing, Z. Yang, W.-H. Zhang and J. Qiu, *Energy Environ. Sci.*, 2013, **6**, 1480–1485.
25 T. Leijtens, G. E. Eperon, S. Pathak, A. Abate, M. M. Lee and H. J. Snaith, *Nat. Commun.*, 2013, **4**, 2885.

